THE JOURNAL OF PHYSICAL CHEMISTRY C

Article

pubs.acs.org/JPCC

Evaluating the Effect of Heteroatoms on the Photophysical Properties of Donor−Acceptor Conjugated Polymers Based on 2,6-Di(thiophen-2-yl)benzo[1,2-b:4,5-b′]difuran: Two-Photon Cross-Section and Ultrafast Time-Resolved Spectroscopy

Ricardo J. Vázquez,[†] Hyungjun Kim,[†] Brandon M. Kobilka,[‡] Benjamin J. Hale,[‡] Malika Jeffries-EL,[‡,§] Paul Zimmerman,[†] and Theodore Goodson, lll*[,†]

[†]Department of Chemistry, University of Michigan, Ann Arbor, Michigan 48109, United States

[‡]Department of Chemistry, Iowa State University, Ames, Iowa 50011, United States

[§]Department of Chemistry and Division of Materials Science, Boston University, Boston, Massachusetts 02215, United States

Supporting Information

ABSTRACT: We investigate the influence of the heteroatom on the electronic and photophysical properties of four conjugated polymers based on 3,7-didodecyl-2,6-di(thiophen-2-yl)benzo[1,2-*b*:4,5-*b*′]difuran (BDF) as the donor and 3,6-di(thiophen-2-yl)-1,4-diketopyrrolo[3,4-*c*]pyrrole (TDPP) or 3,6-di(2-furanyl)-1,4-diketopyrrolo[3,4-*c*]pyrrole (FDPP) as the acceptor. The polymers with a furan as the linker showed higher extinction coefficients than their thiophene counterparts. Ultrafast fluorescence decay showed that the exciton relaxation process is affected by the type of linker in these conjugated polymers. Theoretical calculations showed that the polymers with a furan as the linker are more planar than their thiophene analogues. Also, theoretical calculation showed that the polymers with a thiophene as the linker have larger transition dipole moments. The two-photon absorption cross sections (TPACS) of the polymers with a furan as the linker were larger than their thiophene polymer analogues. These results suggest that the polymers with a furan as the linker have higher charge transfer character than their thiophene polymers analogues. The photovoltaics performance for these polymers are correlated with their optical properties. These results suggest that furan-derivatives are good candidates for synthetic exploration for long-range energy transport materials in photovoltaic applications.

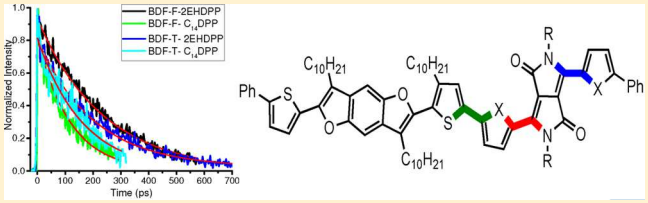

1. INTRODUCTION

The development and use of organic materials is of great interest in the scientific and industrial community due to their potential optoelectronic applications. There has been a great deal of success for the polymers used in solar and light emitting devices.[1,2] Organic polymeric systems such as PTB7 have reached power-conversion efficiencies (PCE) above 10%.[3] Even greater accomplishments in light emitting diode devices has been reported when organic polymers are incorporated as the active material.[4] However, the PCE of photovoltaic devices based on organic polymers have not been able to achieve such a high efficiency as silicon-based photovoltaic devices.[5] The use of conjugated polymers may offer further opportunities in order to enhance the solar cell efficiencies if one can understand the fundamental structure−function relationship which gives rise to the dynamics of the exciton in these systems.[6−16]

There has been reports trying to unravel the electronic and exciton interactions of useful conjugated polymers for solar applications.[17,18] For example, the processes of exciton diffusion (ED), charge transfer (CT), and excitation energy transport (EET) has been thoroughly investigated by a variety of optical and electronic techniques.[19] In the case of ED, the absorption of a photon promotes an entangled interaction between the excited electron and the associated hole in a bound excited state.[20] The interaction between the excited electron and the associated hole (exciton) needs to be broken in order to produce charge carriers that will result in electrical current. Therefore, the ability of the excitons to diffuse in order to arrive the respective interface for exciton splitting is fundamental in the photovoltaic process. This process is known as the exciton diffusion,[21] and it can be studied by using ultra-fast spectroscopy (UFS) and time-resolved fluorescence (TRF) techniques.[9,12,22−24] In electron donor−acceptor polymers, the electrons and holes are weakly localized between the donor−acceptor (D-A) interface; therefore, they are considered as CT excitons.[25,26] The charge transfer character of a system can be evaluate by using nonlinear optics (NLO) such as two-photon absorption (TPA) techniques, which is proportional to the square of the dipole moment.[27−30] Recently, studies have suggested that organic materials with a high dipole moment can

Received: February 22, 2017
Revised: May 19, 2017
Published: June 16, 2017

DOI: 10.1021/acs.jpcc.7b01767
J. Phys. Chem. C 2017, 121, 14382−14392

Table 1. Summary of the Steady-State and Solar Cell Performance of the Investigated Polymers

sample	molecular weight (kDa)	PCE (%)[39]	absorbance λ_{Max} (nm)	ε 10^4 (M^{-1} cm^{-1})	ε/repeating unit 10^4 (M^{-1} cm^{-1})	emission λ_{Max} (nm)	Φ (%)	HOMO/LUMO (eV)[40]
BDF-F-2EHDPP	55.6	2.28	397, 656	113 at 397 nm 313 at 656 nm	2.75 at 397 nm 7.6 at 656 nm	692	6.7	−5.5/−3.7
BDF-F-C_{14}DPP	44.2	2.77	400, 656	67 at 400 nm 168 at 656 nm	2.31 at 400 nm 5.79 at 656 nm	692	3.6	−5.5/−3.8
BDF-T-2EHDPP	24.0	2.10	391, 660	43 at 391 nm 67 at 660 nm	2.52 at 391 nm 3.94 at 660 nm	525, 703	3.5	−5.6/−3.8
BDF-T-C_{14}DPP	8	0.97	406, 670	13 at 406 nm 24 at 670 nm	2.60 at 406 nm 4.8 at 670 nm	560, 695	1.9	−5.6/−3.7

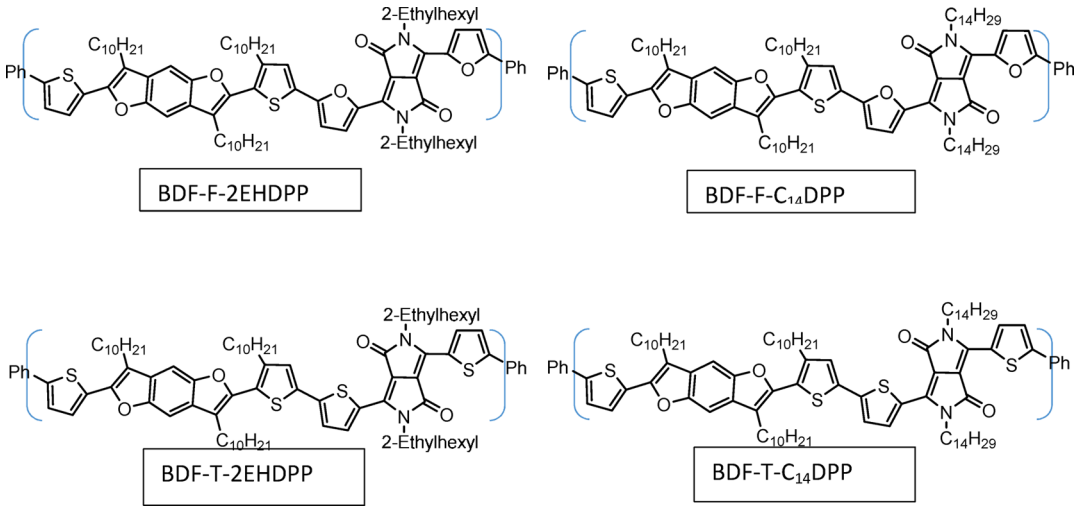

Figure 1. Repeating unit of the investigated polymers. All of the polymers are constituted from a benzodifuran (BDF) unit as the donor, a thiophene or a furan as the linker, and a diketopyrolopyrrolle (DPP) as the acceptor unit. 2-Ethylhexyl or tetradecyl as side chain groups were varied for solubility purposes.[39]

prevent the exciton recombination process.[31] It is also important to have insight into the exciton mechanism of delocalization away from the original absorbing point. The mechanism of delocalization depends on how strong the excitons are coupled within the molecule.[32−34] If the electronic interaction is strong a coherent mechanism dominates, while if the electronic interaction is weak an incoherent hopping-type mechanism dominates.[34−36]

Thiophene derivatives have been widely used as active materials for optoelectronic applications.[37] Recently, efforts to incorporate furan derivatives into main-chains where thiophene derivatives are normally used have emerged.[37,38] In addition to the common isoelectric properties that furan has with thiophene, studies have shown that the incorporation of furan derivatives has an immediate impact in the polymer solubility. From a synthetic point of view, this could mean the possibility of synthesizing polymers with significantly higher molecular weights without the need to have a large or branched alkyl side chain.[39] In solar cell devices, studies have shown a slightly higher PCE (reaching 5%) for polymers that replace thiophene with furan derivatives in their main-chain.[40] Specifically, for the polymers under investigation a 0.18% to 1.31% PCE increase for furan polymers over the thiophene polymer analogues (Table 1) was reported.[39] The furan molecule contains a smaller size atom with a higher electronegativity. It also has been suggested that the less aromaticity of furan in comparison with thiophene could facilitate the formation of quinoidal structures, which could result in the stabilization of the HOMO levels and enhancing the planarity of the polymer.[41] However, a deeper photophysical insight of the exciton behavior in these polymers should be established. By understanding these differences in the exciton dynamics one can explain the higher PCE % reported when a furan is incorporated into the main-chain.

In this report we elucidate the photophysical processes occurring in a selected group of conjugated polymers based on 2,6-di(thiophen-2-yl)benzo[1,2-b:4,5-b′]difurans (BDF) as the donor and diketopyrrolopyrrole (DPP) as the acceptor. The resulting conjugate donor−acceptor polymers are shown in Figure 1. We are most interested in the electronic intermolecular and intramolecular interactions between the donor−acceptor moieties. We investigated the steady-state, time-resolved fluorescence, and non-linear optical properties of these conjugated polymers. We also present electronic structure calculations regarding the electronic states and transition dipole moments in these polymers.

2. EXPERIMENTAL SECTION

2.1. Materials. The polymers investigated in this paper were synthesized via a Stille polycondensation reaction of (5,5′-(3,7-didecylbenzo[1,2-*b*:4,5-*b*′]difuran-2,6-diyl)bis(4-decylthiophene-5,2-diyl))bis(trimethylstannane)[42] and 3,6-bis(5-bromofuran-2-yl)-2,5-bis(2-ethylhexyl)pyrrolo[3,4-*c*]pyrrole-1,4-(2H,5H)-dione, 3,6-bis(5-bromofuran-2-yl)-2,5-bis(tetradecyl)-pyrrolo[3,4-*c*]pyrrole-1,4(2H,5H)-dione, 3,6-di(5-bromo-2-thienyl)-2,5-bis(2-ethylhexyl)pyrrolo[3,4-*c*]pyrrole-1,4-(2*H*,5*H*)-dione or bis(5-bromothiophen-2-yl)-2,5-bis-(tetradecyl)pyrrolo[3,4-*c*]pyrrole-1,4(2H,5H)-dione, respectively.[39] The molecular weights of the polymers were determined using gel permeation chromatography (GPC) at

DOI: 10.1021/acs.jpcc.7b01767
J. Phys. Chem. C 2017, 121, 14382−14392

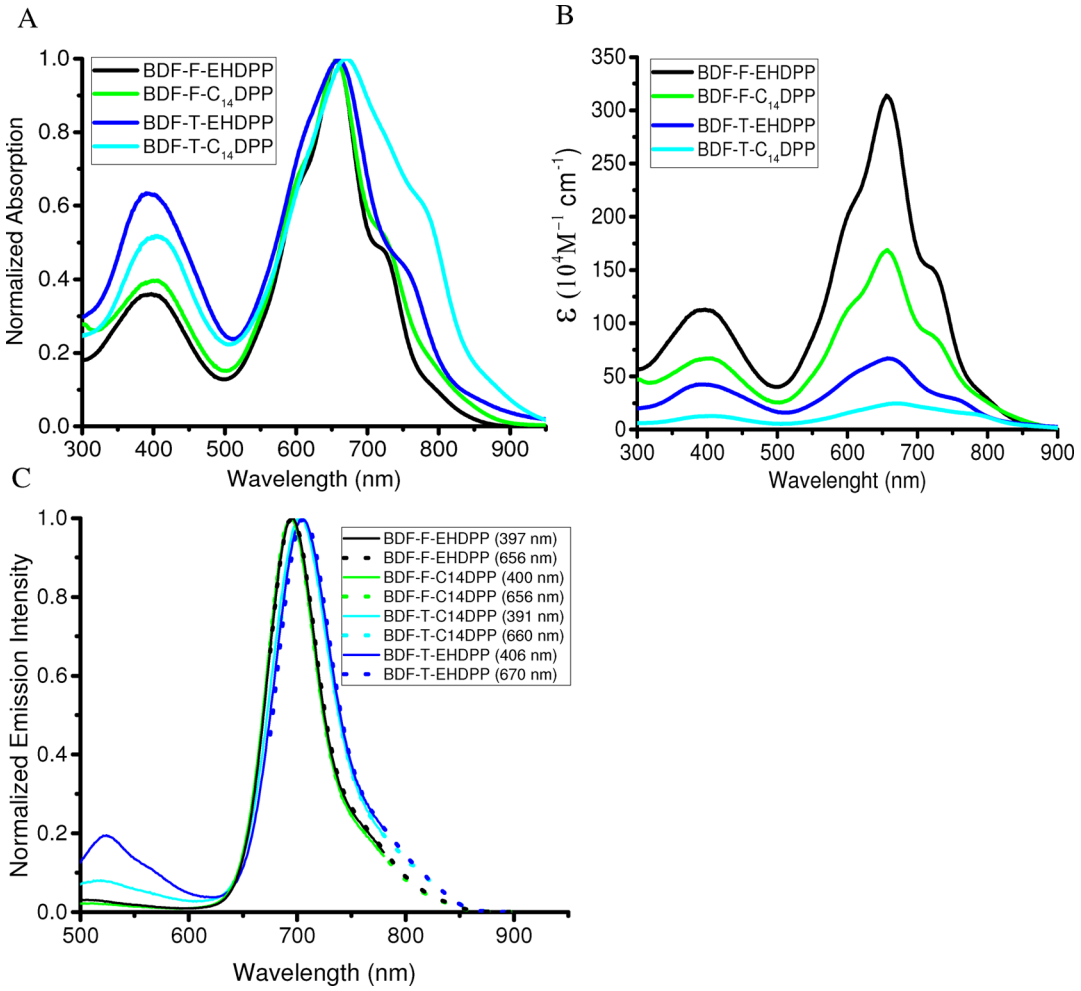

Figure 2. Steady-state spectra of the investigated polymers in chloroform: normalized absorption spectra (A), molar extinction coefficient spectra (B), and normalized emission spectra at different excitation wavelengths (C). Panel C shows the emission spectra when both absorption bands are excited. Interestingly, the polymers show the same emission spectrum regardless of the absorption band that was excited (400 or 650 nm region). The specific excitation wavelength used is shown in the legend.

50 °C using THF as the eluent with a flow rate of 1.0 mL/min. Calibration was based on polystyrene standards.

2.2. Steady-State Measurements. All of the measurements were performed at room temperature. Concentrations ranging from 1.0×10^{-3} to 3.0×10^{-6} M were used for the measurements. The samples were placed in 4 mm quartz cuvettes. Steady-state absorption spectra were measured using an Agilent 8432 UV−visible absorption spectrophotometer. The emission spectrum measurements were performed with a Fluoromax-2 spectrophotometer. Absorption spectra measurements were taken before and after each measurement to ensure that there was no appreciable photodegradation during the fluorescence lifetime or two-photon absorption measurements. The fluorescence quantum yields (Q.Y.) of the samples were calculated using a known procedure,[43,44] and zinc phthalocyanine in toluene (ϕ = 0.3) was used as the standard.[45] The excitation wavelength for the Q.Y. calculation was 650 nm.

2.3. Density Functional Theory Calculation. Theoretical investigation has been performed in order to analyze the experimental results of the two photon absorption cross-section. It is impossible to calculate the electronic structure of the full polymer; therefore, the polymer repeating units have been taken to approximate the polymer's chemical property. The long alkyl chains are replaced by the short chains such as decyl groups ($C_{10}H_{21}$) to methyl groups and phenyl end groups to methyl groups. Also two side chain groups, 2-ethlhexyl and tetradecyl groups ($C_{14}H_{29}$), are simplified to 2-ethylpropyl and butyl groups, respectively, to save computational time without significant effect on the electronic properies. The ground state geometry of each monomer was obtained by computations using density functional theory (DFT). The ωB97X-D functional basis sets are employed.[46,47] The ground state calculations were conducted using Q-Chem 4.0.[48]

Excited state simulations using time-dependent DFT (TDDFT) were performed to analyze the trend of lifetime. The same functional used in the ground state calculations and smaller basis sets, 3-21G*, were employed for the geometry optimization of the first singlet excited state (S_1) in the gas phase. Single-point energy calculations to evaluate the electronic property (Fluorescence emission energy and corresponding transition dipole moment) were performed using 6-31G* basis sets, and the medium effect is included using polarizable continuum. The dielectric constant of dichloromethane is 8.91. All excited state calculations were conducted using Q-Chem 4.0.[48]

2.4. Time-Resolved Fluorescence Measurements. The time-resolved fluorescence experiments were performed using an ultrafast fluorescence up-conversion setup that had

DOI: 10.1021/acs.jpcc.7b01767
J. Phys. Chem. C 2017, 121, 14382−14392

previously been described.[49] A mode-locked Ti-sapphire femtosecond laser (Spectra Physics Tsunami) was used to generate 80 fs pulses at 800 nm wavelength with a repetition rate of 82 MHz. This mode-locked laser was pumped by a 532 nm continuous light output from another laser (Spectra Physics Millennia), which has a gain medium of neodymium-doped yttrium vanadate (Nd:YVO4). A 400 nm excitation pulse was generated by a second harmonic β- barium borate crystal, and the residual 800 nm beam was made to pass through a computer-controlled motorized optical delay line. The polarization of the excitation beam was controlled by a berek compensator. The power of the excitation beam varied between 33 to 36 mW. The fluorescence emitted by the sample was up-converted by a nonlinear crystal of β-barium borate by using the residual 800 nm beam, which had been delayed by the optical delay line with a gate step of 6.25 fs. By this procedure, the measurement of the fluorescence is enabled and can be measured temporally. The monochromator is used to select the wavelength of the up-converted beam of interest, and the selected beam is detected by a photomultiplier tube (R152P, Hamamatsu, Hamamatsu City, Japan). The photomultiplier tube converts the detected beam into photon counts, which can be read from a computer. Coumarin 30, Coumarin 153, and Cresyl Violet dyes were used for calibrating the laser at different collection wavelengths. The instrument response function (IRF) has been determined from the Raman signal of water to have a width of 110 fs.[30] Lifetimes of fluorescence decay were obtained by fitting the fluorescence decay profile to the most accurate fit. Mono and multiexponential decay functions convoluted with IRF in MATLAB and Origin 8 were necessary for the data analysis. The time-correlated single photon counting (TCSPC) technique, which has been described previously, was used to study the long component of the investigated polymers.[50] The laser used for the TCSPC measurement was a Kapteyn Murnane (KM) mode-locked Ti-sapphire laser. The output beam from the KM laser was at 800 nm wavelength, with pulse duration of ∼30 fs. The output beam was frequency-doubled using a nonlinear barium borate crystal to obtain a 400 nm beam. A polarizer was used to vary the power of the 400 nm beam that excites the sample. Focus on the sample cell (quartz cuvette, 0.4 cm path length) was ensured using a lens of focal length 11.5 cm. Collection of fluorescence was done in a direction perpendicular to the incident beam into a monochromator, and the output from the monochromator was coupled to a photomultiplier tube, which converted the photons into counts.

2.5. Two-Photon Excited Fluorescence Measurements. Two-photon spectroscopy was performed using a mode-locked Ti:sapphire laser which is tunable from 700 to 900 nm delivering 110 fs output pulses at a repetition rate of 80 MHz. Emission scans were performed at 830 nm excitation while scanning 690−700 nm emission, but the exact emission detection wavelength during the power dependence scan was selected by the emission wavelength that produced the highest number of counts at 415 nm excitation (by absorbing simultaneously two photons of half of the energy; 830 nm). Rhodamine B was used as the standard. Input power from the laser was varied using a variable neutral density filter. Two-photon power-dependent fluorescence intensity was utilized to determine the two-photon absorption cross section through the two-photon emission fluorescence (TPEF) method.[51]

3. RESULTS

3.1. Synthesis and Molecular Weight Determination. All of the four polymers used in this investigation are based on the electron-donating moiety 3,7-didodecyl-2,6-di(thiophen-2-yl)benzo[1,2-*b*:4,5-*b*′]difuran and the electron-accepting moieties 3,6-di(thiophen-2-yl)-1,4-diketopyrrolo[3,4-*c*]pyrrole or 3,6-di(2-furanyl)-1,4-diketopyrrolo[3,4-*c*]pyrrole. The composition of the conjugated monomers was varied to evaluate the impact of heteroatom substitution on the photophysical properties of the resulting polymers. The length of the side chain on each of the comonomers was also varied to improve the solubility and processabillity of the polymers.

3.2. UV−vis Absorption. Figure 2A shows the normalized steady-state absorption of the investigated polymers. The measurements were recorded from chloroform solutions, and their relevant data are summarized in Table 1. All of the four polymers exhibited two distinct absorption bands as is typical for such electron donor−acceptor polymers.[39,52,53] The absorption maximum of the polymers (near 650 nm) can be attributed to the intermolecular charge transfer between the electron-donating and electron-accepting units, while the small peak (near 400 nm) can be attributed to the localized $\pi-\pi^*$ transition between the BDF and DPP units.[54] A similar behavior has been documented in π-conjugated polymers having similar donor−acceptor interactions.[55] Theoretical calculations of the first and second singlet excitation were conducted, and we were able to corroborate that the high energy transition (S_2) correspond to a $\pi-\pi^*$ transition in the polymer backbone while the low energy transition (S_1) correspond to the charge transfer state between the BDF and PDI units (Figure S8 and Table S9). The core of the absorption for all of the polymers extends in the visible region toward the NIR region, near the peak of the solar flux, making them suitable for photovoltaic applications.[56] The molar extinction coefficient (Figure 2B) is higher for those polymers containing a furan. This could contribute to the reported higher PCE for these polymers.[39]

3.3. Steady-State Fluorescence. The steady-state emission spectra at different excitation wavelengths for the investigated polymers are shown in Figure 2C. The measurements were recorded from chloroform solution, and their relevant data were summarized in Table 1. All of the polymers have a major emissive peak near 700 nm, but the thiophene-containing polymers showed another significant emissive peak near the 550 nm region. As it can be observed in Figure 2C, the emissive band near 700 nm can be accessed by exciting both the near 400 nm and the near 650 nm bands. To address the possibility of self-absorption, we conducted an easy experiment in which we evaluated the emission intensity as a function of wavelength at different concentrations for all of the investigated polymers (Figure S1). The reabsorption phenomena has been documented as a distortion in the emissive band when the emissive band overlap with the absorption band.[57] As can be observed in Figure S1, there is no distortion of the emissive band (near 650 nm) upon increasing the optical density/concentration at the range of optical density/concentration in which the experiments were carried out. This experiment shows no evidence of reabsorption in the investigated materials at the range of optical density/concentration in which the experiments were carried out. In order to have a deeper insight into the absorption bands that contributes to these emissive states the excitation spectra were recorded (Figure S2). As expected,

DOI: 10.1021/acs.jpcc.7b01767
J. Phys. Chem. C 2017, 121, 14382−14392

the excitation spectrum at near 550 nm of the thiophene-containing polymers shows higher intensity than their furan analogues. The quantum yields (Φ) of the investigated polymers are shown in Table 1. The polymers that contain furan showed a relatively higher Φ than their thiophene analogues. It has been suggested that higher Φ values are detrimental to the photovoltaic efficiency due to enhanced radiative decay pathways of the exciton.[36] On the other hand, low quantum yield has been correlated with enhanced nonradiative process. In these polymers, the systems with higher PCE also had higher Φ values. Therefore, other parameters such as exciton relaxation and TPA capabilities must be taken into considerations for the larger PCE obtained.

3.4. Two-Photon Absorption. The two-photon excited fluorescence method was conducted in order to measure the TPA cross-section of the polymers. The results indicate that the polymers with a furan in the main-chain have 1 order of magnitude higher TPA cross-section than their thiophene analogs (Table 2). The TPA cross sections have been strongly

Table 2. Two-Photon Absorption Cross-Section

polymer	TPA cross-section (GM)	TPA cross-section per monomer (GM)
BDF-F-2EHDPP	2790.4	69.76
BDF−F-C14DPP	2183.4	75.2
BDF-T-2EHDPP	205.6	12
BDF-T-C14DPP	109.9	24.00

associated with the charge transfer character of the material.[63] Also, studies have been suggested that the morphology of the materials (planarity) could be an important feature for the TPA nature.[14,64,74] Under these circumstances a higher transition dipole moment suggests a better coupling/interaction between the donor−acceptor junctions. This subsequently will lead to a better energy transfer between the two moieties. These connections were also made with the electronic structure calculations (see below). The DFT calculations showed that the polymers with a furan as the linker have lower dihedral angles between the donor-linker and linker-acceptor junction (Figure 4), thus making them more planar than the thiophene analogues. Our results agree with previous studies, and the TPA cross-section values have a linear relationship with the lower dihedral angles between the donor-linker-acceptor of the polymers. This indicates that the FDPP-containing polymers are more planar, have much better charge separation properties, and have a higher charge transfer character than their corresponding thiophene polymer analogues.[13,27]

The values of the TPA cross-section are reported by polymer and by repeating units. The square dependence of the investigated polymers is evidence in Figure S5.

3.5. Time-Resolved Fluorescence Decay. Up-conversion measurements were carried out in order to investigate the fluorescence lifetime of the polymers. In order to study the fluorescence lifetime component of the donor part (BDT) the instrument was tuned up to detect the 525−560 nm emission wavelength. To study the fluorescence lifetime component of the acceptor part the instrument was tuned up to detect the 693−700 nm emission wavelength. Time correlated single photon counting (TCSPC) experiments were also conducted in order to elucidate the long component of the fluorescence lifetime.[58] A multiexponential decay function was used to fit the fluorescence lifetime dynamics of the BDT unit while a monoexponential decay function was used to fit the DPP exciton lifetime dynamics, and the relevant data are summarized in Table 3.

The measured fluorescence lifetime of the polymers in this study are similar to previously reported fluorescence lifetime dynamics of conjugated polymers based on thiophene derivatives as the donor and DPP as the acceptor.[36,58] Our measurements showed a slower fluorescence lifetime dynamics for the polymers with furan as the linker. If we evaluate the effect of the side chain in the acceptor's fluorescence lifetime, the polymers with the 2-ethylhexyl as the side chains have almost two times slower decay dynamics than their analogs with the 14 carbons as a side chain (Table 3). Specifically, the up-conversion data showed that the fast first decay relaxation process for the near 550 nm emissive band (coming from the donor) of the polymers was unaffected by the type of linker nor by the side chain type. Whereas, the polymers with furan as the linker showed a slower second components fluorescence decay lifetime than their thiophene analogs.

The same trend was observed for the up-conversion measurements of the near 650 nm emission band (acceptor part). The polymers with a furan molecule as the linker showed a longer fluorescence lifetime. Theoretical calculations (see below) show that the polymers with a thiophene in their main-chain have a larger transition dipole moment. The rate of radiative decay (Γ) for an isolated molecule is proportional to the cube of emission energy (ΔE) and the square of the corresponding transition dipole moment.[61,62] Giving that they have almost identical band gap energies (emission energy), we attributed these shorter lifetime dynamics by the polymers with a thiophene in their main-chain due to their larger transition dipole moment. Interestingly, only the polymers with the 2-ethylhexyl as a side chain exhibited a measurable rise time in the up-conversion profile. This is evidence of an energy transfer process from the donor moiety to the acceptor moiety. The lack of a rise time in the polymers with a linear side chain could be due to a faster energy transfer that overlaps with the IRF of

Table 3. Ultra-Fast Excited State Lifetime Dynamics

	fluorescence up-conversion							TCSPC
	525−560 nm region				600−700 nm region			
compound	A_1	T_1 (ps)	A_2	T_2 (ps)	A_1	T_1 (ps)	rise time (fs)	T_1 (ps)
BDF-F-EHDPP	0.73	4.33	0.49	296	0.95	233	500 (rise time)	757
BDF-F-C_{14}DPP	0.97	4.87	0.29	250	0.82	119	n/a (IRF)	406
BDF-T-EHDPP	1.0	4.35	0.29	178	0.80	220	250 (rise time)	628
BDF-T-C_{14}DPP	0.84	6.36	0.29	174	0.83	160	n/a (IRF)	354

DOI: 10.1021/acs.jpcc.7b01767
J. Phys. Chem. C 2017, 121, 14382−14392

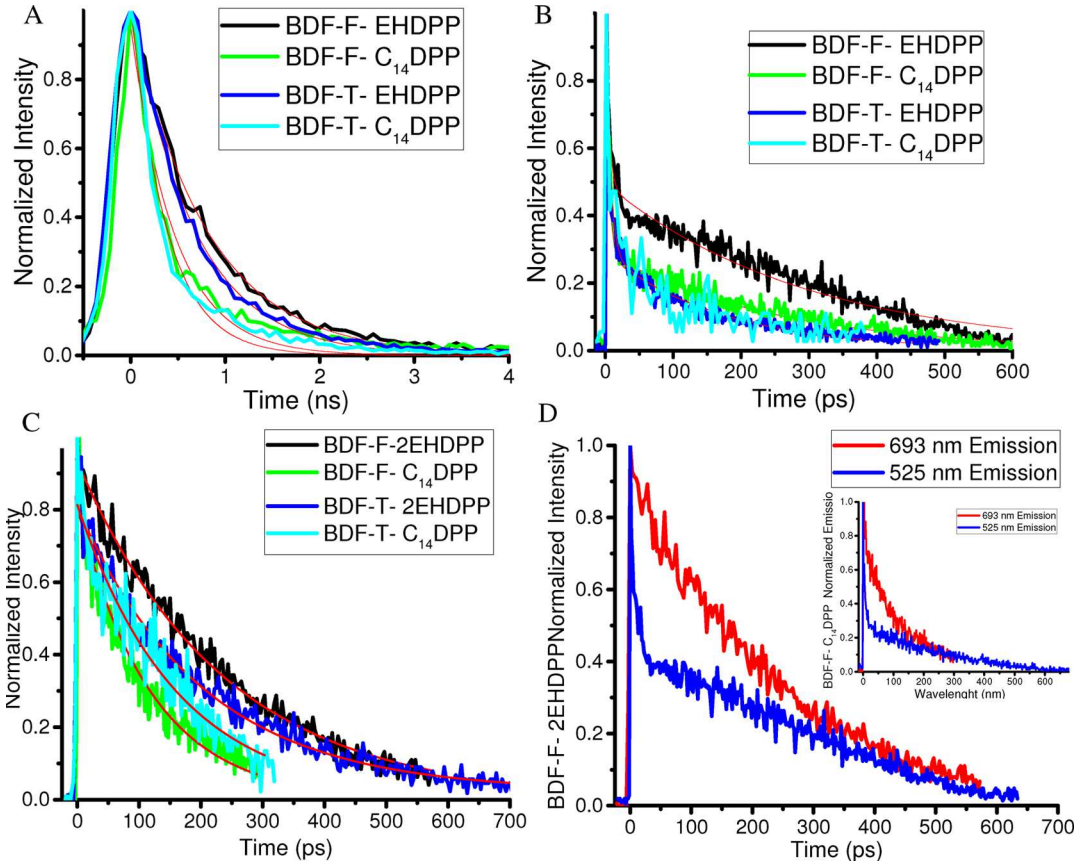

Figure 3. Fluorescence lifetime of the investigated polymers. The TCSPC setup was used to investigate the fluorescence long component by the acceptor at the 690−700nm region (A). The fluorescence Up-Conversion set-up were used to investigate the short components of both, the donor at 525−560nm (B) and the acceptor 690−700nm (C) emission region. Using the BDF-F-2EHDPP and the BDF-F-C_{14}DPP polymers as an example of the difference between the excited state fluorescence lifetime decay profile between the donor and the acceptor (D). For the donors, the Fluorescence Up-Conversion data were collected at 525 nm for all of the investigated polymers but 560 nm emission were used for the BDF-T-C_{14}DPP polymer.

the instrument. This result indicates that the donor is able to delocalize energy along the linkers which enhance energy transfer between the donor moiety and the acceptor moiety.[59,70−73] The same trend was observed with the TCSPC data (Table 3). A slower long-decay component for the polymers with furan as the linker was observed. The faster lifetime decay dynamics reported for the polymers with thiophene as the linker are in agreement with a higher transition dipole moment.[60,61]

The fluorescence lifetime of the investigated polymers were measured by using the fluorescence up-conversion technique and the time correlated single photon counting (TCSPC) technique. Fluorescence lifetime in the 525−560 nm (donor) exhibits a two component decay while the fluorescence lifetime dynamics in the 600−700 nm region (acceptor) exhibits a single component lifetime decay. The UPC and the TCSPC lifetime measurements of the 600−700 nm emissive band do not match in value but they match in the tendency of the lifetime. This is because the UPC resolution is in the short picoseconds range while the TCSPC goes to the microsecond range. Thus, the long component measurements by the TCSPC are more accurate.

3.6. Density Functional Theory Calculations of the Investigated Polymers. The optimized structures of the four repeating units are displayed in Figure S3, and corresponding *xyz* coordinates are listed in the Supporting Information (Table S10). The previous work of Pond et al.[58] shows that the molecular planarity is very important to determine the TPA cross section.[62] In this study, three dihedral angles are measured to quantify the planarity of optimized monomer structures: two dihedral angles involving nitrogen atoms bonded to side chains in DPP (red and blue one in Figure 4B) and one dihedral angle of donor/acceptor interface (green one in Figure 4B). There is a noticeable difference in the dihedral angles depending on the type of linker on the polymer. For the polymer with the thiophene as a linker, the sulfur atom has a much larger atomic radius than the oxygen atom in the furan linker, and this causes severe steric hindrance with adjacent carbonyl groups in DPP. This results in relatively large distortion at the donor/acceptor interface (green one in Figure 3) for the thiophene linker, 28.3° and 23.6° for BDF-T-2EHDPP and BDF-T-C_{14}DPP, respectively. In contrast to that, polymers with furan as linkers remain almost planar with dihedral angle values of 3.5° and 4.7° for BDF-F-2EHDPP and BDF-F-C_{14}DPP, respectively. The size effects are obviously observed in the other two dihedral angles, too. (Table S6 in the Supporting Information)

The type of linker as well as the type of alkyl side chains affects dihedral angles within the DPP group, especially for the thiophene linker. Compared to the linear chain tetradecyl groups, the branched alkyl groups, 2-ethylhexyl, induce high geometric restrain. The geometric effects of the 2-ethyl branch

DOI: 10.1021/acs.jpcc.7b01767
J. Phys. Chem. C 2017, 121, 14382−14392

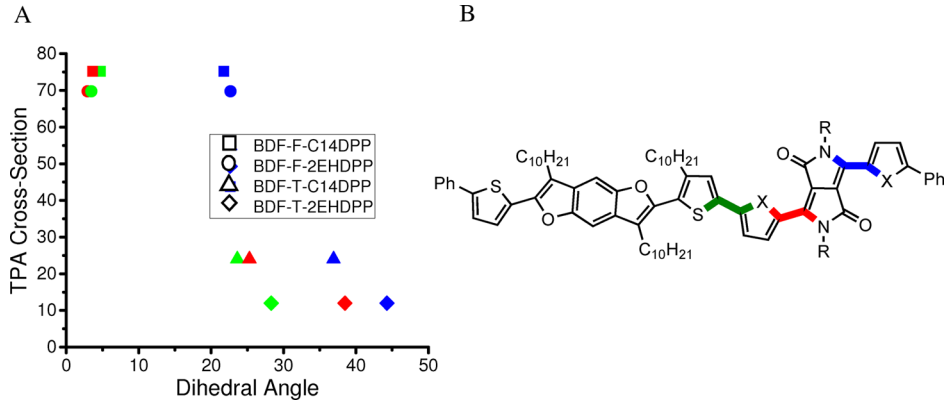

Figure 4. (A) Linear correlation between the TPA cross section and individual dihedral angles (square: BDF-F-C14DPP, circle: BDF-F-2EHDPP, triangle: BDF-T-C14DPP, diamond: BDF-T-2EHDPP, color code of each dihedral angle value is corresponding to the ones in panel B). (B) Selected three dihedral angles to measure the planarity of monomers.

are measured to increase the dihedral angles by 13.2° and 7.4° than the chain groups for the dihedral angle in red and blue color, respectively. The effect of alkyl side chain on the planarity is negligible for the furan linker. The dependence of alkyl side chain effect on the type of linker group can be explained as follows. The breaking of planarity due to the large size of the sulfur atom causes repulsion between side chain and linker groups, and this repulsion enhances the distortion more. The furan linker does not affect the planarity, and repulsion between side chain and linker groups is avoidable. We have found a linear correlation between the planarity of the polymers and the two photon absorption cross-section: the more planar (the smaller dihedral angle), the higher the cross section (Figure 4A).

The rate of radiative decay (Γ) for an isolated molecule is proportional to the cube of emission energy (ΔE) and the square of corresponding transition dipole moment (μ_{tr}). The predicted emission energy of the four monomers is almost the same (Table 2).[61,62] This outcome is in line with the result of the electrochemical study which gives almost invariant HOMO/LUMO level depending on the type of monomer (Table 1). The transition dipole moment of the thiophene linker, however, is larger than the one of the furan linker by more than 1 D. The analogy with a classical dipole moment model gives that the larger transition dipole moment of the thiophene linkers comes from the longer monomer length due to the widening at the donor/acceptor interface.

The approximated rates based on these predictions are listed in Table 4. The four data points are severely scattered, and no linear correlation is found. A closer examination, however, reveals that TDDFT simulations can explain the faster radiative decaying of the thiophene linker than the furan linker within the same alkyl side chain, with a similar driving force and a larger transition dipole moment. The reason why the simulations fail to give linear correlation might be due to the omission of nonradiative decay pathways. The comparison of quantum yield (Table 1) between side chains for the same linker group shows that the quantum yield of the tetradecyl side chain is almost half of the 2-ethylhexyl group's one. This implies that the contribution of nonradiative decay is larger for the tetradecyl side chain. The consideration of a nonradiative decay pathway might be necessary to give a linear correlation.

Table 4. Predicted Emission Energy (eV), Transition Dipole Moment (D), Rate of Radiative Decay (Arbitrary Unit), and Lifetime (ps) of the Four Monomers of Interest

	ΔE	μ_{tr}	Γ	lifetime
BDF-F-2EHDPP	2.23	4.98	273.15	757
BDF-F-C_{14}DPP	2.15	4.74	222.03	406
BDF-T-2EHDPP	2.19	6.05	386.0	628
BDF-T-C_{14}DPP	2.18	6.12	390.2	354

4. DISCUSSION

The aim of this study was to probe and correlate the photophysical properties of four new conjugated polymers with their respective photovoltaic performance. The polymers, but those that have a furan as the linker between the donor and the acceptor moieties, showed higher molar extinction coefficients. Organic materials with high extinction coefficients are important for both (1) the device fabrication and (2) creation of charge carriers.[63] Organic materials with a higher extinction coefficient will promote the development of lightweight and more flexible devices.[63] Furthermore, harvesting more photons is proportional to the generation of free carrier concentrations which could result in higher PCE.[36]

It has been reported that BDF derivatives in either solution or in the solid state emit in the 400−500 nm spectral region.[64] Interestingly, our measured emission spectrum showed a more intense emission band near 550 nm for those polymers containing thiophene as the linkers. This increase in the emission intensity is likely due to a weaker electronic interaction between the BDF and the DPP than their furan analogues.[58] On the other hand, the lower emission intensity near 550 nm by the polymers with a furan as the linker suggests that a more efficient energy transfer process could be happening. The TPA cross-section was measured and the data shows a larger TPA cross-section by the polymer with a furan molecule in their main-chain. This data indicates a better communication between the donor and acceptor units for those polymers that have a furan as a linker in their main-chain. With the power of a pulsed laser, we can easily excite the materials and detect the near 550 nm emission band for all of the investigated polymer via the up-conversion fluorescence technique (Figure 4B and Table 3). As can be observed in Table 3, longer lifetime dynamics was measured for those polymers that have furan as a linker by detecting both near 550 nm and near 650 nm wavelengths. The same trend was observed for the long component lifetimes measured by the

DOI: 10.1021/acs.jpcc.7b01767
J. Phys. Chem. C 2017, 121, 14382−14392

time correlated single photon counting. This agreement in the fluorescence lifetime in both emissive band and by using two different instruments suggest that the emissive bands of the near 550 nm are not artificial. The fluorescence quantum yields were measured and the furan-containing polymers have relatively higher quantum yields than the thiophene-containing polymers analogs. Studies have shown higher quantum yield values for monomers/molecules with a thiophene in their backbone over their furan analogs. These monomers have shown triplet character and results have been explained by the possible heavy atom effect by the thiophene containing materials over the furan analogues.[65] In this study, the polymer with a furan molecule in the main-chain showed higher quantum yield. We attributed these slightly higher quantum yields from the polymers with a furan molecule in their main-chain due to a better energy transfer from the donor to the acceptor over their thiophene analogs. Further studies in order to evaluate the charge transfer character of the materials were conducted and are discussed below.

Previous studies have tried to elucidate the exciton lifetime for thiophene and furan derivatives. A multiexponential excitonic lifetime behavior has been documented for materials based on furan or thiophene derivatives.[66] In the case of electron donor−acceptor systems, distyrylfurans have shown slower excitonic lifetimes than their distyrylthiophenes analogues.[67] We found longer fluorescence lifetime for the polymers with a furan molecule as the linker than their thiophene analogues. The rate of radiative decay (Γ) for an isolated molecule is proportional to the cube of emission energy (ΔE) and the square of corresponding transition dipole moment.[61,62] Our theoretical calculations showed that the polymers with a thiophene molecule in their main-chain have a larger transition dipole moment than the furan analogues. As aforementioned, given that our polymers have almost identical ΔE, this data suggest that the fluorescence lifetime of the investigated polymers can be explained by the transition dipole moment. The polymers with a furan molecule in their main-chain have a longer fluorescence lifetime than their thiophene analogues due to their shorter transition dipole moment. This discrepancy in the exciton lifetime may play a role in the reported enhanced PCE by the polymers with a furan in their main-chain. In solar cell devices, the fluorescence lifetime is proportional to the exciton diffusion length.[68] Longer fluorescence decay suggests more time for the exciton to reach the respective interface for subsequent exciton splitting, resulting in the generation of more charge carriers for photovoltaic conversion.

The TPEF techniques allow us to determine the two-photon absorption cross sections of the polymers. The polymers with a furan molecule as the linker showed larger two-photon absorption cross sections compared to their thiophene polymer analogues. This indicates a better charge separation between the donor and the acceptor leading to a potential higher charge carrier generation.[75,36] It has been documented that the morphology of a material may play an important role in the two photon cross-section value.[11] The DFT calculations showed that the polymers with a furan as the linker have lower dihedral angles between the donor-linker and linker-acceptor junction (Figure 4A and Table S6), thus making them more planar than the thiophene polymer analogues. As mentioned above, under these circumstances a larger TPA cross section suggests a better coupling/communication between the donor−acceptor junctions. This subsequently will lead to a better energy transfer between the two moieties. Previous reports have demonstrated that an enhanced two photon absorption cross-section may play a role in preventing the exciton recombination process.[69] We believe that the dipole moment of the molecule can interact with the entanglement of the exciton and decrease the Coulombic interactions. This will result in easier exciton splitting for subsequent charge carrier generation.

5. CONCLUSIONS

We have investigated the photophysical properties of four conjugated polymers based on benzodifuran (BDF) as the donor and diketopyrrolopyrrole (DPP) as the acceptor by modifying the proximity of a furan or a thiophene as linkers to the DPP acceptor unit. All of the polymers absorb in the visible spectral region. The polymers with a furan molecule incorporated to the main-chain showed a higher extinction coefficient than their thiophene polymer analogs. Ultrafast spectroscopy showed that the polymers with a furan molecule in their main-chain have longer fluorescence lifetimes. The two-photon excited fluorescence measurements showed that the polymers with a furan molecule in their main-chain have a larger TPA cross-section than their thiophene analogs. Theoretical calculation showed that the polymers with a thiophene molecule in their main-chain have a larger transition dipole moment than their furan analogues. The TD-DFT calculations were also correlated with the TPA cross-section, and there is a linear relationship between the TPA cross-section and the dihedral angles between the donor-linker-acceptor junctions of the investigated polymers, indicating that the planarity of the polymer plays an important role in the ability of a material to absorb subsequently two-photons and, consequently, in the charge transfer character of the polymer.

For the investigated polymers, our results further demonstrated that the incorporation of a furan molecule into polymers backbones that are typically dominated by thiophenes can have an impact in the photophysical properties of the polymers. The bigger extinction coefficient by the polymers with a furan as the linker could result in the creation of more charge carriers due to a higher excited state population. The longer fluorescence lifetime by the polymers with a furan as the linker can be beneficial for achieving a longer exciton diffusion length, which can result in more excitons arriving the interface for exciton splitting. The TD-DFT shows that the polymers with a furan as the linker have lower dihedral angles between the donor-linker-acceptor junctions. These results agree with previous studies, and the polymers with a more planarity showed the bigger TPA cross section than their polymer analogues. The combination of the TD-DFT calculations and the TPA cross-section values demonstrate the importance of the morphology for the charge transfer character and the subsequence photovoltaic performance of a material. All of the aforementioned electronic processes could be contributing and can explain the slightly larger PCE reported for those polymers with a furan as the linker, thus suggesting that furan derivatives could be advantageous for synthetic exploration in order to develop materials with long-range energy transport for photovoltaic applications.

■ ASSOCIATED CONTENT

Supporting Information

The Supporting Information is available free of charge on the ACS Publications website at DOI: 10.1021/acs.jpcc.7b01767.

DOI: 10.1021/acs.jpcc.7b01767
J. Phys. Chem. C 2017, 121, 14382−14392

(1) Emission spectrum at different concentrations; (2) excitation spectrum; (3) optimized structure of the investigated polymers; (4) rise time of the near 650 nm emission band; (5) two-photon character of the investigated polymers; (6) dihedral angles between de donor-linker-acceptor-linker junctions; (7) molecular orbital distribution; (8) electronic transition diagram; (9) theoretical excitation energy and corresponding main transitions; and (10) Cartesian coordinates of the optimized structures. (PDF)

AUTHOR INFORMATION

Corresponding Author

*E-mail: tgoodson@umich.edu.

ORCID

Hyungjun Kim: 0000-0002-7204-3718

Theodore Goodson III: 0000-0003-2453-2290

Notes

The authors declare no competing financial interest.

ACKNOWLEDGMENTS

This material is based upon work supported by the U.S. Department of Energy, Office of Science, Office of Basic Energy Sciences, Photochemistry, via Grant DE-SC0012482.

REFERENCES

(1) Guo, X.; Baumgarten, M.; Müllen, K. Designing π-Conjugated Polymers for Organic Electronics. *Prog. Polym. Sci.* **2013**, *38*, 1832−1908.

(2) Bildirir, H.; Gregoriou, V.; Avgeropoulos, A.; Scherf, U.; Chochos, C. L. Porous Organic Polymers as Emerging New Materials for Organic Photovoltaic Applications: Current Status and Future Challenges. *Mater. Horiz.* **2017**, DOI: 10.1039/C6MH00570E.

(3) Chen, J. D.; Cui, C.; Li, Y. Q.; Zhou, L.; Ou, Q. D.; Li, C.; Tang, J. X. Single-Junction Polymer Solar Cells Exceeding 10% Power Conversion Efficiency. *Adv. Mater.* **2015**, *27*, 1035−1041.

(4) Coe-Sullivan, S. Optoelectronics: Quantum Dot Developments. *Nat. Photonics* **2009**, *3*, 315−316.

(5) Green, M. A.; Emery, K.; Hishikawa, Y.; Warta, W.; Dunlop, E. D. Solar Cell Efficiency Tables (Version 45). *Prog. Photovoltaics* **2015**, *23*, 1−9.

(6) Furgal, J. C.; Jung, J. H.; Goodson, T.; Laine, R. M. Analyzing Structure-Photophysical Property Relationships for Isolated T8, T10, and T12 Stilbenevinylsilsesquioxanes. *J. Am. Chem. Soc.* **2013**, *135*, 12259−12269.

(7) Donehue, J. E.; Varnavski, O. P.; Cemborski, R.; Iyoda, M.; Goodson, T. Probing Coherence in Synthetic Cyclic Light-Harvesting Pigments. *J. Am. Chem. Soc.* **2011**, *133*, 4819−4828.

(8) Bhaskar, A.; Ramakrishna, G.; Lu, Z.; Twieg, R.; Hales, J. M.; Hagan, D. J.; Goodson, T. Investigation of Two-Photon Absorption Properties in Branched Alkene and Alkyne Chromophores. *J. Am. Chem. Soc.* **2006**, *128*, 11840−11849.

(9) Guo, M.; Varnavski, O.; Narayanan, A.; Mongin, O.; Majoral, J. P.; Blanchard-Desce, M.; Goodson, T. Investigations of Energy Migration in an Organic Dendrimer Macromolecule for Sensory Signal Amplification. *J. Phys. Chem. A* **2009**, *113*, 4763−4771.

(10) Varnavski, O. P.; Ostrowski, J. C.; Sukhomlinova, L.; Twieg, R. J.; Bazan, G. C.; Goodson, T. Coherent Effects in Energy Transport in Model Dendritic Structures Investigated by Ultrafast Fluorescence Anisotropy Spectroscopy. *J. Am. Chem. Soc.* **2002**, *124*, 1736−1743.

(11) Raymond, J. E.; Bhaskar, A.; Goodson, T.; Makiuchi, N.; Ogawa, K.; Kobuke, Y. Synthesis and Two-Photon Absorption Enhancement of Porphyrin Macrocycles. *J. Am. Chem. Soc.* **2008**, *130*, 17212−17213.

(12) Goodson, T. Optical Excitations in Organic Dendrimers Investigated by Time-Resolved and Nonlinear Optical Spectroscopy. *Acc. Chem. Res.* **2005**, *38*, 99−107.

(13) Ramakrishna, G.; Goodson, T.; Rogers-Haley, J. E.; Cooper, T. M.; McLean, D. G.; Urbas, A. Ultrafast Intersystem Crossing: Excited State Dynamics of Platinum Acetylide Complexes. *J. Phys. Chem. C* **2009**, *113*, 1060−1066.

(14) Bhaskar, A.; Guda, R.; Haley, M. M.; Goodson, T. Building Symmetric Two-Dimensional Two-Photon Materials. *J. Am. Chem. Soc.* **2006**, *128*, 13972−13973.

(15) Goodson, T. Time-Resolved Spectroscopy of Organic Dendrimers and Branched Chromophores. *Annu. Rev. Phys. Chem.* **2005**, *56*, 581−603.

(16) Ispasoiu, R. G.; Balogh, L.; Varnavski, O. P.; Tomalia, D. A.; Goodson, T. Large Optical Limiting and Ultrafast Luminescence Dynamics from Novel Metal-Dendrimer Nanocomposite Materials. *J. Am. Chem. Soc.* **2000**, *122*, 11005−11006.

(17) Dou, L.; Liu, Y.; Hong, Z.; Li, G.; Yang, Y. Low-Bandgap Near-IR Conjugated Polymers/Molecules for Organic Electronics. *Chem. Rev.* **2015**, *115*, 12633−12665.

(18) Gélinas, S.; Rao, A.; Kumar, A.; Smith, S. L.; Chin, A. W.; Clark, J.; Friend, R. H. Ultrafast Long-Range Charge Separation in Organic Semiconductor Photovoltaic Diodes. *Science* **2014**, *343*, 512−516.

(19) Cho, H. S.; Rhee, H.; Song, J. K.; Min, C. K.; Takase, M.; Aratani, N.; Kim, D. Excitation Energy Transport Processes of Porphyrin Monomer, Dimer, Cyclic Trimer, and Hexamer Probed by Ultrafast Fluorescence Anisotropy Decay. *J. Am. Chem. Soc.* **2003**, *125*, 5849−5860.

(20) Luhman, W. A.; Holmes, R. J. Enhanced Exciton Diffusion in an Organic Photovoltaic Cell by Energy Transfer Using a Phosphorescent Sensitizer. *Appl. Phys. Lett.* **2009**, *94*, 153304.

(21) Pivrikas, A.; Sariciftci, N. S.; Juška, G.; Österbacka, R. A Review of Charge Transport and Recombination in Polymer/Fullerene Organic Solar Cells. *Prog. Photovoltaics* **2007**, *15*, 677−696.

(22) Varnavski, O.; Ispasoiu, R. G.; Balogh, L.; Tomalia, D.; Goodson, T. Ultrafast Time-Resolved Photoluminescence From Novel Metal-Dendrimer Nanocomposites. *J. Chem. Phys.* **2001**, *114*, 1962−1965.

(23) Keller, J. M.; Glusac, K. D.; Danilov, E. O.; McIlroy, S.; Sreearuothai, P.; Cook, A.; Schanze, K. S. Negative Polaron and Triplet Exciton Diffusion in Organometallic "Molecular Wires. *J. Am. Chem. Soc.* **2011**, *133*, 11289−11298.

(24) Kazaoui, S.; Minami, N.; Tanabe, Y.; Byrne, H. J.; Eilmes, A.; Petelenz, P. Comprehensive Analysis of Intermolecular Charge-Transfer Excited States in C_{60} and C_{70} films. *Phys. Rev. B: Condens. Matter Mater. Phys.* **1998**, *58*, 7689.

(25) Veldman, D.; Meskers, S. C.; Janssen, R. A. The Energy of Charge-Transfer States in Electron Donor-Acceptor Blends: Insight into the Energy Losses in Organic Solar Cells. *Adv. Funct. Mater.* **2009**, *19*, 1939−1948.

(26) Wong, W. Y.; Wang, X. Z.; He, Z.; Djurišić, A. B.; Yip, C. T.; Cheung, K. Y.; Chan, W. K. Metallated Conjugated Polymers as a New Avenue Towards High-Efficiency Polymer Solar Cells. *Nat. Mater.* **2007**, *6*, 521−527.

(27) Ramakrishna, G.; Varnavski, O.; Kim, J.; Lee, D.; Goodson, T. Quantum-Sized Gold Clusters as Efficient Two-Photon Absorbers. *J. Am. Chem. Soc.* **2008**, *130*, 5032−5033.

(28) Devadas, M. S.; Kim, J.; Sinn, E.; Lee, D.; Goodson, T.; Ramakrishna, G. Unique Ultrafast Visible Luminescence in Monolayer-Protected Au_{25} clusters. *J. Phys. Chem. C* **2010**, *114*, 22417−22423.

(29) Lahankar, S. A.; West, R.; Varnavski, O.; Xie, X.; Goodson, T.; Sukhomlinova, L.; Twieg, R. Electronic Interactions in a Branched Chromophore Investigated by Nonlinear Optical and Time-Resolved Spectroscopy. *J. Chem. Phys.* **2004**, *120*, 337−344.

(30) Flynn, D. C.; Ramakrishna, G.; Yang, H. B.; Northrop, B. H.; Stang, P. J.; Goodson, T. Ultrafast Optical Excitations in Supramolecular Metallacycles with Charge Transfer Properties. *J. Am. Chem. Soc.* **2010**, *132*, 1348−1358.

DOI: 10.1021/acs.jpcc.7b01767
J. Phys. Chem. C 2017, 121, 14382−14392

(31) Carsten, B.; Szarko, J. M.; Son, H. J.; Wang, W.; Lu, L.; He, F.; Rolczynski, B. S.; Lou, S. J.; Chen, L. X.; Yu, L. Examining the Effect of the Dipole Moment on Charge Separation in Donor-Acceptor Polymers for Organic Photovoltaic Applications. *J. Am. Chem. Soc.* **2011**, *133*, 20468−20475.
(32) Wang, Y.; Ranasinghe, M. I.; Goodson, T. Ultrafast Fluorescence Investigation of Excitation Energy Transfer in Different Dendritic Core Branched Structures. *J. Am. Chem. Soc.* **2003**, *125*, 9562−9563.
(33) Varnavski, O.; Samuel, I. D.W.; Pålsson, L. O.; Beavington, R.; Burn, P. L.; Goodson, T. Investigations of Excitation Energy Transfer and Intramolecular Interactions in a Nitrogen Corded Distrylbenzene Dendrimer System. *J. Chem. Phys.* **2002**, *116*, 8893−8903.
(34) Ranasinghe, M. I.; Varnavski, O. P.; Pawlas, J.; Hauck, S. I.; Louie, J.; Hartwig, J. F.; Goodson, T. Femtosecond Excitation Energy Transport in Triarylamine Dendrimers. *J. Am. Chem. Soc.* **2002**, *124*, 6520−6521.
(35) Varnavski, O. P.; Goodson, T.; Mohamed, M. B.; El-Sayed, M. A. Femtosecond excitation dynamics in gold nanospheres and nanorods. *Phys. Rev. B: Condens. Matter Mater. Phys.* **2005**, *72* (23), 235405.
(36) Keller, B.; McLean, A.; Kim, B. G.; Chung, K.; Kim, J.; Goodson, T. Ultrafast Spectroscopic Study of Donor-Acceptor Benzodithiophene Light Harvesting Organic Conjugated Polymers. *J. Phys. Chem. C* **2016**, *120*, 9088−9096.
(37) Saadeh, H.; Goodson, T.; Yu, L. Synthesis of a Polyphenylene-co-Furan and Polyphenylene-co-Thiophene and Comparison of their Electroluminescent Properties. *Macromolecules* **1997**, *30*, 4608−4612.
(38) Yamamoto, T.; Zhou, Z.; Kanbara, T.; Shimura, M.; Kizu, K.; Maruyama, T.; Nakamura, Y.; Fukuda, T.; Lee, B.-L.; Ooba, N.; Tomaru, S.; Kurihara, T.; Kaino, T.; Kubota, K.; Sasaki, S. π-Conjugated Donor-Acceptor Copolymers Constituted of π-Excessive and π-Deficient Arylene Units. Optical and Electrochemical Properties in Relation to CT Structure of the Polymer. *J. Am. Chem. Soc.* **1996**, *118*, 10389−10399.
(39) Kobilka, B. M.; Hale, B. J.; Ewan, M. D.; Dubrovskiy, A. V.; Nelson, T. L.; Duzhko, V.; Jeffries-EL, M. Influence of Heteroatoms on Photovoltaic Performance of Donor-Acceptor Copolymers Based on 2, 6-di(Thiophen-2-yl)Benzo [1, 2-b: 4, 5-b′] Difurans and Diketopyrrolopyrrole. *Polym. Chem.* **2013**, *4*, 5329.
(40) Woo, C. H.; Beaujuge, P. M.; Holcombe, T. W.; Lee, O. P.; Fréchet, J. M. Incorporation of Furan into Low Band-Gap Polymers for Efficient Solar Cells. *J. Am. Chem. Soc.* **2010**, *132*, 15547−15549.
(41) Huo, L.; Huang, Y.; Fan, B.; Guo, X.; Jing, Y.; Zhang, M.; Li, Y.; Hou, J. Synthesis of a 4,8-Dialkoxy-Benzo[1,2-b:4,5-b′]diFuran unit and its Application in Photovoltaic Polymer. *Chem. Commun.* **2012**, *48*, 3318−3320.
(42) Kobilka, B. M.; Dubrovskiy, A. V.; Ewan, M. D.; Tomlinson, A. L.; Larock, R. C.; Chaudhary, S.; Jeffries-EL, M. Synthesis of 3, 7-diiodo-2, 6-di(Thiophen-2-yl)Benzo [1, 2-b: 4, 5-b′] diFurans: Functional Building Blocks for the Design of New Conjugated Polymers. *Chem. Commun.* **2012**, *48*, 8919−8921.
(43) Furgal, J. C.; Jung, J. H.; Goodson, T.; Laine, R. M. Analyzing Structure-Photophysical Property Relationships for Isolated T8, T10, and T12 Stilbenevinylsilsesquioxanes. *J. Am. Chem. Soc.* **2013**, *135*, 12259−12269.
(44) Maciejewski, A.; Steer, R. P. Spectral and Photophysical Properties of 9, 10-Diphenylanthracene in Perfluoro-n-Hexane: the Influence of Solute-Solvent Interactions. *J. Photochem.* **1986**, *35*, 59−69.
(45) Adegoke, O. O.; Ince, M.; Mishra, A.; Green, A.; Varnavski, O.; Martínez-Díaz, M. V.; Goodson, T. Synthesis and Ultrafast Time Resolved Spectroscopy of Peripherally Functionalized Zinc Phthalocyanine Bearing Oligothienylene-ethynylene Subunits. *J. Phys. Chem. C* **2013**, *117*, 20912−20918.
(46) Chai, J. D.; Head-Gordon, M. Long-Range Corrected Hybrid Density Functionals with Damped Atom-Atom Dispersion Corrections. *Phys. Chem. Chem. Phys.* **2008**, *10*, 6615−6620.
(47) Chai, J. D.; Head-Gordon, M. Systematic Optimization of Long-Range Corrected Hybrid Density Functionals. *J. Chem. Phys.* **2008**, *128*, 084106.
(48) Shao, Y.; et al. Advances in Molecular Quantum Chemistry Contained in the Q-Chem 4 Program Package. *Mol. Phys.* **2015**, *113*, 184−215.
(49) Varnavski, O.; Samuel, I. D. W.; Pålsson, L. O.; Beavington, R.; Burn, P. L.; Goodson, T. Investigations of Excitation Energy Transfer and Intramolecular Interactions in a Nitrogen Corded Distrylbenzene Dendrimer System. *J. Chem. Phys.* **2002**, *116*, 8893−8903.
(50) Ramakrishna, G.; Bhaskar, A.; Goodson, T. Ultrafast Excited State Relaxation Dynamics of Branched Donor-π-Acceptor Chromophore: Evidence of a Charge-Delocalized State. *J. Phys. Chem. B* **2006**, *110*, 20872−20878.
(51) Chi, C. Y.; Chen, M. C.; Liaw, D. J.; Wu, H. Y.; Huang, Y. C.; Tai, Y. A Bifunctional Copolymer Additive to Utilize Photoenergy Transfer and to Improve Hole Mobility for Organic Ternary Bulk-Heterojunction Solar Cell. *ACS Appl. Mater. Interfaces* **2014**, *6*, 12119−12125.
(52) Li, W.; Roelofs, W. S.; Turbiez, M.; Wienk, M. M.; Janssen, R. A. Polymer Solar Cells with Diketopyrrolopyrrole Conjugated Polymers as the Electron Donor and Electron Acceptor. *Adv. Mater.* **2014**, *26*, 3304−3309.
(53) Lin, H. W.; Lee, W. Y.; Chen, W. C. Selenophene-DPP Donor-Acceptor Conjugated Polymer for High Performance Ambipolar Field Effect Transistor and Nonvolatile Memory Applications. *J. Mater. Chem.* **2012**, *22*, 2120−2128.
(54) Huang, P.; Du, J.; Gunathilake, S. S.; Rainbolt, E. A.; Murphy, J. W.; Black, K. T.; Biewer, M. C. Benzodifuran and Benzodithiophene Donor-Acceptor Polymers for Bulk Heterojunction Solar Cells. *J. Mater. Chem. A* **2015**, *3*, 6980−6989.
(55) Beaujuge, P. M.; Amb, C. M.; Reynolds, J. R. Spectral Engineering in π-Conjugated Polymers with Intramolecular Donor-Acceptor Interactions. *Acc. Chem. Res.* **2010**, *43*, 1396−1407.
(56) Liang, Y.; Xu, Z.; Xia, J.; Tsai, S. T.; Wu, Y.; Li, G.; Yu, L. For the Bright Future-Bulk Heterojunction Polymer Solar Cells with Power Conversion Efficiency of 7.4%. *Adv. Mater.* **2010**, *22*, E135−E138.
(57) Davis, N. J.; Francisco, J.; Tabachnyk, M.; Richter, J. M.; Lamboll, R. D.; Booker, E. P.; Rivarola, F. W. R.; Griffiths, J. T.; Ducati, C.; Menke, S. M.; Deschler, F. Photon Reabsorption in Mixed CsPbCl3: CsPbI3 Perovskite Nanocrystal Films for Light-Emitting Diodes. *J. Phys. Chem. C* **2017**, *121*, 3790.
(58) Adegoke, O. O.; Jung, I. H.; Orr, M.; Yu, L.; Goodson, T. Effect of Acceptor Strength on Optical and Electronic Properties in Conjugated Polymers for Solar Applications. *J. Am. Chem. Soc.* **2015**, *137*, 5759−5769.
(59) Brédas, J. L.; Beljonne, D.; Coropceanu, V.; Cornil, J. Charge-Transfer and Energy-Transfer Processes in π-Conjugated Oligomers and Polymers: a Molecular Picture. *Chem. Rev.* **2004**, *104*, 4971−5004.
(60) Luo, Y.; Xu, Y.; Zhang, W.; Li, W.; Li, M.; He, R.; Shen, W. Theoretical Insights into the Phosphorescence Quantum Yields of Cyclometalated (C∧C*) Platinum (II) NHC Complexes: π-Conjugation Controls the Radiative and Nonradiative Decay Processes. *J. Phys. Chem. C* **2016**, *120*, 3462−3471.
(61) Caricato, M.; Andreussi, O.; Corni, S. Semiempirical (ZINDO-PCM) Approach to Predict the Radiative and Nonradiative Decay Rates of a Molecule Close to Metal Particles. *J. Phys. Chem. B* **2006**, *110*, 16652−16659.
(62) Pond, S. J.; Rumi, M.; Levin, M. D.; Parker, T. C.; Beljonne, D.; Day, M. W.; Brédas, J. L.; Marder, S. R.; Perry, J. W. One-and Two-Photon Spectroscopy of Donor-Acceptor-Donor Distyrylbenzene Derivatives: Effect of Cyano Substitution and Distortion from Planarity. *J. Phys. Chem. A* **2002**, *106*, 11470−11480.
(63) Wang, Q.; Zhang, S.; Xu, B.; Ye, L.; Yao, H.; Cui, Y.; Hou, J. Effectively Improving Extinction Coefficient of Benzodithiophene and Benzodithiophenedione-Based Photovoltaic Polymer by Grafting Alkylthio Functional Groups. *Chem. - Asian J.* **2016**, *11*, 2650−2655.

DOI: 10.1021/acs.jpcc.7b01767
J. Phys. Chem. C 2017, 121, 14382−14392

(64) Mitsui, C.; Tsuji, H.; Sato, Y.; Nakamura, E. Carbazolyl Benzo [1, 2-b: 4, 5-b′] Difuran: An Ambipolar Host Material for Full-Color Organic Light-Emitting Diodes. *Chem. - Asian J.* **2012**, *7*, 1443−1450.
(65) Ohulchanskyy, T. Y.; Donnelly, D. J.; Detty, M. R.; Prasad, P. N. Heteroatom Substitution Induced Changes in Excited-State Photophysics and Singlet Oxygen Generation in Chalcogenoxanthylium Dyes: Effect of Sulfur and Selenium Substitutions. *J. Phys. Chem. B* **2004**, *108*, 8668−8672.
(66) Kamada, K.; Ueda, M.; Ohta, K.; Wang, Y.; Ushida, K.; Tominaga, Y. Molecular dynamics of Thiophene Homologues Investigated by Femtosecond Optical Kerr Effect and Low Frequency Raman Scattering Spectroscopies. *J. Chem. Phys.* **1998**, *109*, 10948−10957.
(67) Carlotti, B.; Kikaš, I.; Škorić, I.; Spalletti, A.; Elisei, F. Photophysics of Push−Pull Distyrylfurans, Thiophenes and Pyridines by Fast and Ultrafast Techniques. *ChemPhysChem* **2013**, *14*, 970−981.
(68) Günes, S.; Neugebauer, H.; Sariciftci, N. S. Conjugated Polymer-Based Organic Solar Cells. *Chem. Rev.* **2007**, *107*, 1324−1338.
(69) Carsten, B.; Szarko, J. M.; Son, H. J.; Wang, W.; Lu, L.; He, F.; Yu, L. Examining the Effect of the Dipole Moment on Charge Separation in Donor-Acceptor Polymers for Organic Photovoltaic Applications. *J. Am. Chem. Soc.* **2011**, *133*, 20468−20475.
(70) Laine, R. M.; Sulaiman, S.; Brick, C.; Roll, M.; Tamaki, R.; Asuncion, M. Z.; Neurock, M.; Filhol, J. S.; Lee, C. Y.; Zhang, J.; Goodson, T. Synthesis and Photophysical Properties of Stilbeneoctasilsesquioxanes. Emission Behavior Coupled with Theoretical Modeling Studies Suggest a 3-D Excited State Involving the Silica Core. *J. Am. Chem. Soc.* **2010**, *132*, 3708−3722.
(71) Yau, S. H.; Varnavski, O.; Gilbertson, J. D.; Chandler, B.; Ramakrishna, G.; Goodson, T. Ultrafast Optical Study of Small Gold Monolayer Protected Clusters: a Closer Look at Emission. *J. Phys. Chem. C* **2010**, *114*, 15979−15985.
(72) Yan, X.; Goodson, T.; Imaoka, T.; Yamamoto, K. Up-Converted Emission in a Series of Phenylazomethine Dendrimers with a Porphyrin Core. *J. Phys. Chem. B* **2005**, *109*, 9321−9329.
(73) Wang, X.; Mader, M. M.; Toth, J. E.; Yu, X.; Jin, N.; Campbell, R. M.; Smallwood, J. K.; Christe, M. E.; Chatterjee, A.; Goodson, T.; Vlahos, C. J. Complete Inhibition of Anisomycin and UV Radiation But Not Cytokine Induced JNK and p38 Activation by an Aryl-Substituted Dihydropyrrolopyrazole Quinoline and Mixed Lineage Kinase 7 Small Interfering RNA. *J. Biol. Chem.* **2005**, *280*, 19298−19305.
(74) Bhaskar, A.; Ramakrishna, G.; Twieg, R. J.; Goodson, T. Zinc Sensing Via Enhancement of Two-Photon Excited Fluorescence. *J. Phys. Chem. C* **2007**, *111*, 14607−14611.
(75) Guo, M.; Varnavski, O.; Narayanan, A.; Mongin, O.; Majoral, J. P.; Blanchard-Desce, M.; Goodson, T. Investigations of Energy Migration in an Organic Dendrimer Macromolecule for Sensory Signal Amplification. *J. Phys. Chem. A* **2009**, *113*, 4763−4771.

DOI: 10.1021/acs.jpcc.7b01767
J. Phys. Chem. C 2017, 121, 14382−14392